Synthesis and Characterization of Composite Flocculant PAFS–CPAM for the Treatment of Textile Dye Wastewater

Yongjun Sun,[1] Huaili Zheng,[1] Mingzhuo Tan,[2] Yili Wang,[3] Xiaomin Tang,[1] Li Feng,[1] Xinyi Xiang[1]

[1]Key laboratory of the Three Gorges Reservoir Region's Eco-Environment, State Ministry of Education, Chongqing University, Chongqing, 400045, China
[2]GuangDong Wealth Environmental Protection Co., Ltd., Guangdong, 529000, China
[3]3College of environmental science and engineering, Beijing Forestry University, Beijing, 100083, China
Correspondence to: H. Zheng (E-mail: zhl@cqu.edu.cn)

ABSTRACT: In this study, a new composite flocculant was prepared by premixing polymeric aluminum ferric sulfate (PAFS) with cationic polyacrylamide (CPAM) to treat textile dye wastewater. Fourier transform infrared spectroscopy (FTIR) and scanning electron microscopy (SEM) were conducted to investigate the structure and morphology of the PAFS–CPAM. The effects of flocculant dosage, initial pH of textile dye wastewater, and settling time after flocculation on the removal of turbidity and chemical oxygen demand (COD) were examined. The flocculation efficiency of PAFS–CPAM for dye treatment was compared with PAFS, CPAM, PAFS/CPAM (PAFS followed by CPAM), and CPAM/PAFS (CPAM followed by PAFS). The synergy of PAFS and CPAM increased the $(Fe–Al)_b$ species of PAFS–CPAM. Treatment with PAFS–CPAM was more effective in removing turbidity and COD than PAFS, CPAM, PAFS/CPAM, and CPAM/PAFS. The turbidity and COD removal rates of textile wastewater were higher than 80 and 90% in the pH range of 5.5 to 8.5, respectively. Furthermore, PAFS–CPAM demonstrated excellent performance in reducing sludge volume after flocculation. © 2013 Wiley Periodicals, Inc. J. Appl. Polym. Sci. **2014**, *131*, 40062.

INTRODUCTION

Textile industries consume huge amounts of water and generate wastewater that needs treatment to meet legislative requirements before being discharged. The wastewater discharge from textile and dye industries are highly contaminated with suspended solids (SSs), chemical oxygen demand (COD), biochemical oxygen demand (BOD), heat, acids, bases, turbidity, and other toxic substances. A large number of conventional decolorization methods such as physico-chemical, chemical, and biological processes have been well established in previous studies. New techniques such as sonochemical process or advanced oxidation have also emerged.[1,2] However, no economically and technically viable method for solving the aforementioned problem has been proposed, and two or three methods are usually needed to achieve an adequate level of COD removal.[3,4] The coagulation–flocculation process is one of the most employed methods in the world for various sludge amounts. The mechanism of the coagulant applied for the COD removal of textile dye wastewater is unclear, and flocculation is an effective method for the removal of COD and turbidity. Flocculation efficiency for textile dye wastewater treatment mostly depends on the chemical characteristics of the flocculants.

Novel coagulants have been extensively studied in recent years. Dual polymer systems have attracted increasing attention because of their superior flocculation efficiency.[5] Dual polymer systems are generally composed of inorganic and organic polymers. In the traditional method of using dual polymer systems, inorganic and organic coagulants are separately added to wastewater. This dual polymer system requires two coagulant addition systems, thus increasing water treatment costs. Therefore, a new method of using dual polymer systems was developed, i.e., inorganic flocculant is premixed with an organic coagulant before the coagulant is used to treat wastewater. This new dual polymer system is called a composite inorganic–organic floccculant. Organic polymeric flocculants, such as cationic polyacrylamide (CPAM) and poly(dimethyl diallylammonium chloride) (PDMDAAC), are used to prepare inorganic–organic composite flocculants. By adding CPAM in the inorganic–organic flocculant, the adsorption-bridging mechanism can be enhanced, thus improving aggregating capacity.[6] Although dual polymer systems have been studied and used widely, limited studies has been conducted on composite inorganic–organic flocculants. The characteristics of composite inorganic–organic flocculants

Table I. Influence of Fe/CPAM Mass Ratio on the Fe–Al Species Distribution of PAFS–CPAM

Flocculant abbreviation	Fe/CPAM mass ratio	Fe–Al species distribution (%)				Turbidity removal (%)	COD removal (%)
		Total iron mass fraction (%)	$(Fe-Al)_a$	$(Fe-Al)_b$	$(Fe-Al)_c$		
PAFS	Without CPAM	12.14	34.63	5.32	60.05	87.9	79.5
PAFS–CPAM6	60 : 1	12.08	41.92	17.26	40.82	93.2	84.4
PAFS–CPAM4	40 : 1	11.72	42.85	20.31	36.84	96.9	86.5

differ from the characteristics of individual inorganic and organic coagulants. Therefore, investigating the characteristic, flocculation behavior, and flocculation efficiency of composite inorganic–organic flocculants is necessary.

In this study, a new inorganic–organic composite coagulant (PAFS–CPAM) was used to treat textile dye water. PAFS–CPAM was prepared by mixing PAFS with CPAM. Considering that reports on the structure, species distribution, and flocculation behavior of composite flocculants are limited, this research aims to investigate these parameters. First, the possible chemical bonds and morphology of PAFS–CPAM were observed by Fourier transform infrared spectroscopy (FTIR) and scanning electron microscopy (SEM). Second, the species distribution of PAFS–CPAM was investigated by the ferron method. Finally, the potency of PAFS–CPAM in treating textile wastewater was verified. The effects of flocculant dosage, initial pH, and settling time on turbidity and COD removal after the flocculation of textile dye wastewater were also examined. The flocculation efficiency results of the wastewater treated with composite flocculant PAFS–CPAM were compared with wastewater with PAFS, CPAM, PAFS/CPAM (PAFS followed by CPAM), and CPAM/PAFS (CPAM followed by PAFS).

EXPERIMENTAL

Materials

All reagents used in this study were of analytical grade except for ferrous sulfate ($FeSO_4 \cdot 7H_2O$) (Molecular Weight (M_W): 278.01, CAS: 7782-63-0), which was of technical grade. Other experimental reagents include concentrated HNO_3 (M_W: 63.01, CAS: 7697-37-2), H_2SO_4 (M_W: 98.08, CAS: 7664-93-9), H_3PO_4 (M_W: 98.00, CAS: 7664-38-2), HCl (M_W: 36.46, CAS: 7647-01-0), and NaOH (M_W: 40.00, CAS: 1310-73-2). All aqueous and standard solutions were prepared with deionized water. All reagents were purchase from Chongqing Chuandong Chemical (group) Co All reagents were used in the experiment without further purification.

Flocculant Preparation

The PAFS used in this study was prepared in our laboratory. The synthetic method and synthetic process are detailed in our previous works.[7,8] CPAM were obtained from HaiXia Chemical Co (China). The intrinsic viscosity of CPAM was 2.35 dL g^{-1} and its cationic degree was 35%. PAFS–CPAM was prepared by PAFS and CPAM. A measured amount of CPAM was injected into the stock solution of PAFS with vigorous stirring at 60°C for 30 min. Thereafter, PAFS–CPAM was obtained as a chestnut-thick liquid. The properties of PAFS–CPAM did not

change in 5 months. The major physicochemical properties of the laboratory-prepared composite flocculants are shown in Table I, and the contents of PAFS and CPAM in the prepared PAFS/CPAM, CPAM/PAFS, and PAFS–CPAM were shown in Table III.

PAFS was added in the rapid mixing phase followed by CPAM after 0.5 min. This dual coagulant was denoted PAFS/CPAM. The reverse addition sequence of PAFS and CPAM was denoted CPAM/PAFS.

The mass ratio of Fe and CPAM was 40 : 1 in the two dual coagulants (PAFS/CPAM and CPAM/PAFS). The dosages of different coagulants were calculated by the quantity of their effective component, i.e., PAFS by Fe, CPAM by its dry weight, and PAFS–CPAM by Fe, and CPAM dry weight.

Flocculant Characterization

FTIR spectra were recorded by using 550 Series II IR spectrometer (BRUKER, Switzerland) with KBr pellets, and polymer morphology was examined by using VEGAIILMU scanning electron microscope (TES-CAN, Czech). The elemental analysis (Elemental Analyzer Vario ELIII, Germany; Element Analyzer Alpha4000) was used to investigate the content of PAFS and CPAM in the prepared PAFS–CPAM. The specific surface area was also determined by Micropore Analyzer (Micropore Analyzer ASAP2020M).

Ferron Analysis

The distribution of Fe–Al species in flocculants was determined by using a timed complexation spectroscopy method that involved the reaction between PAFS and a ferron reagent (8-hydroxy-7-iodoquinoline-5-sulfonic acid). The detailed description of this method can be found in previous studies.[8,9] A brief description is provided as follows. Ultraviolet light absorbance was measured as a function of time at a wavelength of 360 nm to quantify the amount of the formed Fe–Al complex. The reactions of Fe–Al monomeric species with ferron were completed within 1 min [denoted as $(Fe-Al)_a$]. The reaction in the next 3h was conducted for polymeric species $(Fe-Al)_b$.[10] Any Fe–Al that

Table II. The Contents of PAFS and CPAM in the Prepared PAFS/CPAM, CPAM/PAFS, and PAFS–CPAM

Percentage (%)	PAFS/ CPAM	CPAM/ PAFS	PAFS– CPAM4	PAFS– CPAM6
PAFS	97.56	97.56	97.78	98.49
CPAM	2.44	2.44	2.22	1.51

remained unreactive after 3 h was considered precipitated (Fe–Al)$_c$.

Wastewater Characteristics

The textile dye wastewater tested in this study was obtained from Jinyang Textile Co. (China). The wastewater colored with dark blue was highly contaminated with SSs, COD, heat, and other toxic substances. Raw wastewater was filtered by using graticule mesh to remove all large particles and was characterized by measuring the turbidity and COD. The wastewater chemical analysis showed that the turbidity, COD, and pH values were 125 NTU to 137 NTU, 1114 mg·L^{-1} to 1350 mg·L^{-1}, and pH 7.4 to pH 7.9, respectively.

Flocculation Experiments

All coagulation experiments were conducted in 1.0 L Plexiglass beakers by using a program-controlled jar-test apparatus (ZR4–6, Zhongrun Water Industry Technology Development Co., China) at room temperature. The pH of textile dye wastewater was adjusted with HCl (1.0 mol·L^{-1}) or NaOH (1.0 mol·L^{-1}). During the rapid stirring phase (150 rpm), a measured amount of coagulant was pipetted into the wastewater sample (1.0 L). The wastewater samples were mixed rapidly at 150 rpm for 3 min after dosing, followed by slow stirring at 60 rpm for 8 min, and sedimentation for 15 min. After sedimentation, the supernatant samples were collected at 2 cm below the water surface of the tested water sample to measure turbidity (2100Q turbidimeter, HACH) and COD (DR/5000 UV spectrophotometer, HACH).

RESULTS AND DISCUSSION

FTIR Analysis

To investigate the interaction between PAFS and CPAM, the FTIR spectra of PAFS, PAFS–CPAM, and CPAM were obtained (Figure 1). Figure 1(a) shows the FTIR spectrum of CPAM. Strong absorption peaks were observed at 3448.1 and 1165.9 cm^{-1}, which originated from the strong stretching vibration of the amino and carbonyl groups of amide in acrylamide, respectively. The bending vibration absorption peaks of the quaternary ammonium groups appeared at 1664.1 cm^{-1}.[11] Figure 1(c) showed a broad absorption peak for PAFS at 3385.0 cm^{-1} and was attributed to the stretching vibration of the —OH groups. The medium peak at 1633.7 cm^{-1} was assigned to the bending vibration of the —OH groups in the water molecule, i.e., the H—O—H angle distortion frequency, thus indicating that PAFS contained structural and adsorbed water. The FTIR spectral studies revealed that the characteristic absorption peak for sulfate was evident in the range of 900–1200 cm^{-1}. The absorption at 597.9 and 2357 cm^{-1} might be assigned to the Al—O—Al bond stretching vibration and Fe–O–Fe bond bending vibrations.[8,12] The peaks of PAFS were similar to the peaks of PAFS–CPAM, except that extra peaks appeared at 1230.5, 1141.8, 1076.2, and 999.1 cm^{-1} in the PAFS spectra. As shown in Figure 1(b), the shift of peak in PAFS–CPAM at 1638.2 cm^{-1} could be indicative of the interactions between Fe–Al species and CPAM molecules, such as hydrogen bonding and electrostatic interactions, which result in the formation of composite species. It is possible that in these interactions the amino groups of CPAM and the —O— or —OH— groups of Fe–Al species were
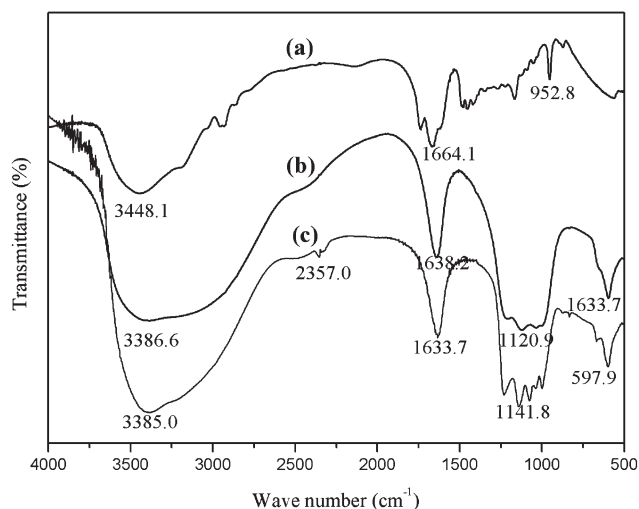

Figure 1. FTIR spectra of (a) CPAM, (b) PAFS–CPAM, and (c) PAFS.

involved, thus indicating the complex formation of PAFS and CPAM.

SEM Analysis

Figure 2 shows the morphology of (a) PAFS, (b) CPAM, and (c) PAFS–CPAM. This observation was supported by the SEM results. CPAM showed a compact and smooth surface morphology. PAFS behaved as an amorphous material and randomly formed aggregates of various sizes and shapes. PAFS was significantly smaller than CPAM at 50 μm and exhibited a curl slice and compact network structure at 10 μm. Figure 2(c) shows that PAFS–CPAM exhibited a fluffy and wrinkled surface structure. The specific surface area of CPAM, PAFS, and PAFS–CPAM were 3.12, 1.69, and 1.87 m^2·g^{-1}, respectively. The specific surface area of PAFS–CPAM was higher than PAFS. These characteristics were favorable in the flocculation of colloidal particles and the formation of bridge aggregation among flocs.[13] The structure of PAFS–CPAM was better than a smooth structure for the adsorption-bridging behavior between flocculants and particles in wastewater treatment.[14] Figure 2 also shows the linear correlation between the logarithms of perimeter (L) and area (A). According to the calculated results for fractal dimension by Image-Pro Plus 6.0,[15,16] the average fractal dimensions of PAFS, CPAM, and PAFS–CPAM were 1.535, 1.247, and 1.151, respectively. The difference in the average fractal dimension presented different morphological structures, thus indicating different physical properties.

Ferron Analysis

Flocculation activity largely depended on the Fe(III) and Al(III) hydrolysis species for ferric salt coagulants. The Fe(III) and Al(III) species in the PAFS–CPAM and PAFS solutions measured and calculated by using the ferron method are shown in Table I. Previous studies showed that a ferron reagent could not react with CPAM.[17] The addition of CPAM gradually increased the (Fe–Al)$_a$ and (Fe–Al)$_b$ species contents but decreased the (Fe–Al)$_c$ species content. The alteration of the Fe–Al species distribution indicated the interaction between the quaternary amino groups in the CPAM molecules and Fe–Al species. The addition of CPAM also increased the stability of the composite
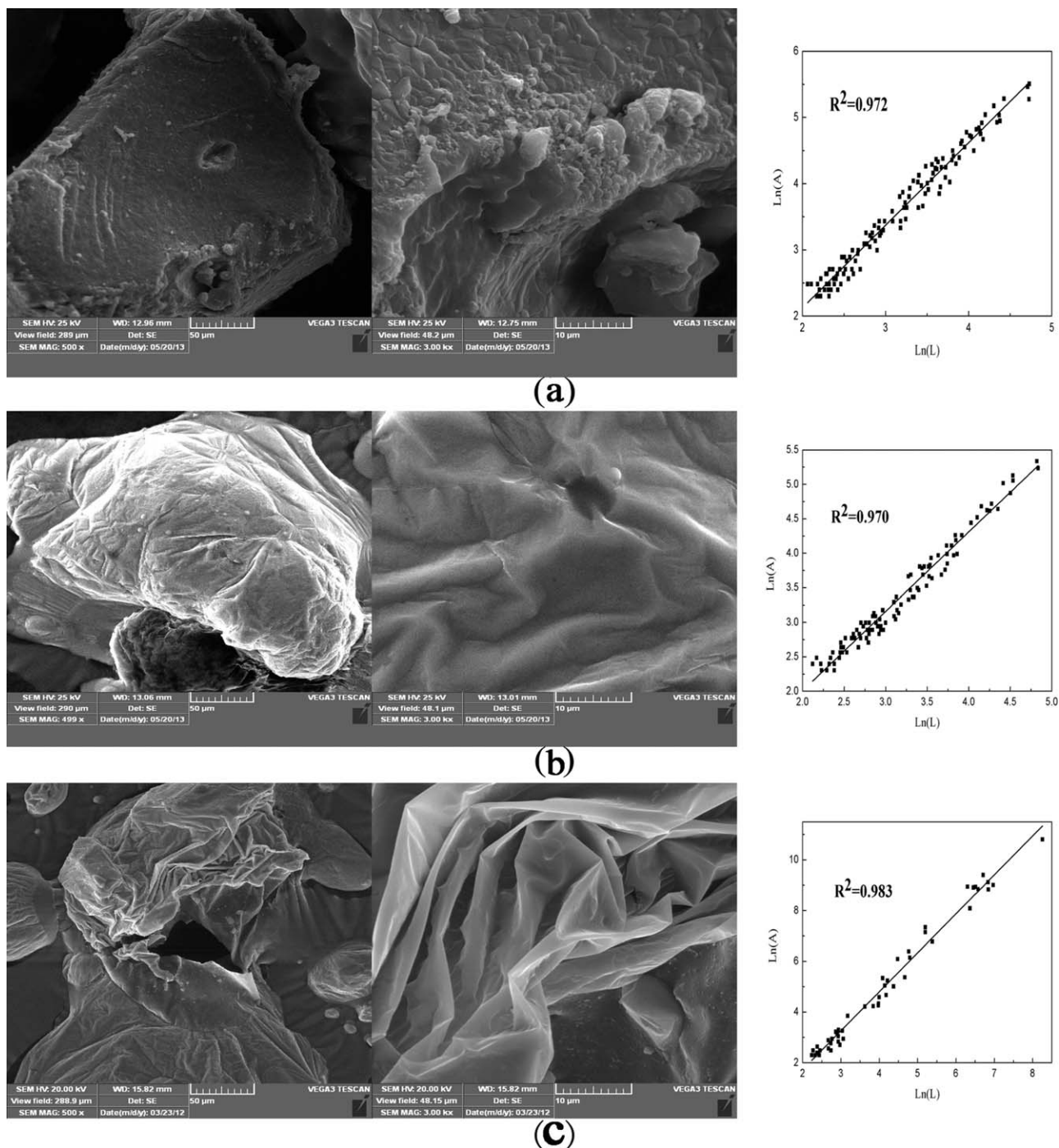
Figure 2. SEM photographs of (a) CPAM, (b) PAFS–CPAM, and (c) PAFS.

flocculant (PFAS–CPAM). Zhu et al.[18] also reported that the addition of CPAM increased the monomeric $(Fe–Al)_a$ species and medium-sized $(Fe–Al)_b$ polymerized species but decreased the large $(Fe–Al)_c$ polymerized species. Coagulation–flocculation performance decreased with high $(Fe–Al)_c$ species content.[8] In contrast, at low $(Fe–Al)_c$ species content, flocculation efficiency increased with increasing $(Fe–Al)_b$ species content. Thus, an appropriate combination of $(Fe–Al)_c$ and $(Fe–Al)_b$ species capable of improving flocculation efficiency could be adopted.[19]

Dosage Effect on Flocculation Efficiency

The flocculation efficiency of PAFS, CPAM, PAFS/CPAM, CPAM/PAFS, PAFS–CPAM6, and PAFS–CPAM4 were compared in terms of turbidity and COD removal. Turbidity removal was consistent with COD removal for all flocculants (Figures 3 and 4). The turbidity and COD removal rates of the six flocculants gradually increased with increasing flocculant dosages and then slightly decreased. In a low dosage range, the flocculation efficiency of CPAM was significantly lower than the flocculation
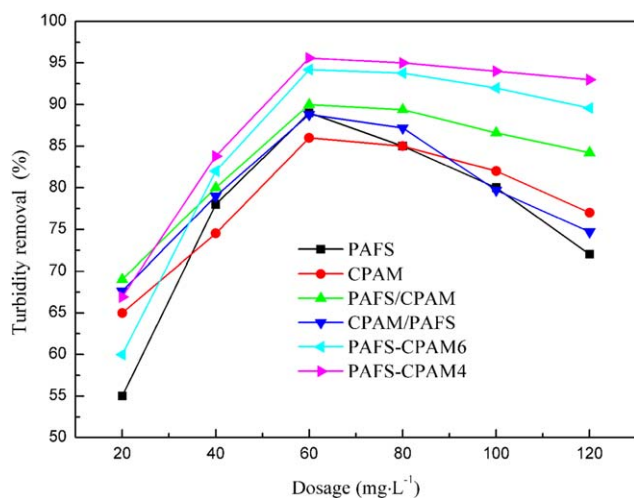
Figure 3. Effect of dosage on turbidity removal. [Color figure can be viewed in the online issue, which is available at wileyonlinelibrary.com.]

Figure 5. Effect of pH on turbidity removal. [Color figure can be viewed in the online issue, which is available at wileyonlinelibrary.com.]

efficiency of other flocculants. Only approximately 65% turbidity and 64% COD could be removed even at a dosage of 20 mg/L. PAFS exhibited a better flocculation effect than CPAM within the dosage range of 40–80 mg/L. When PAFS was used in conjunction with CPAM (PAFS–CPAM), turbidity and COD removal rates improved within the dosage range of 40–120 mg/L (Figures 3 and 4). This result was consistent with a previous research that showed that high removal performance could be achieved when a polymer was used with a conventional flocculant.[20] The difference between the flocculation efficiencies of PAFS/CPAM and CPAM/PAFS was insignificant. The flocculation efficiencies of single and dual flocculants had the following order: PAFS–CPAM4 > PAFS–CPAM6 > PAFS/CPAM > CPAM/ PAFS > PAFS > CPAM. Although no differences were found between the quantities of PAFS and CPM for PAFS–CPAM6, PAFS/CPAM, and CPAM/PAFS, the dosing method affected the performance of these three dual coagulants. Figures 3 and 4 also show that PAFS–CPAM6 was more effective than PAFS/CPAM and CPAM/PAFS within the dosage range of 40–120 mg/L.
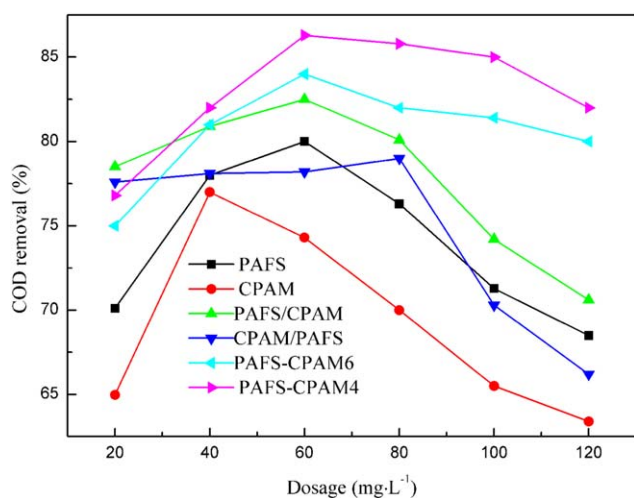

Figure 4. Effect of dosage on COD removal. [Color figure can be viewed in the online issue, which is available at wileyonlinelibrary.com.]
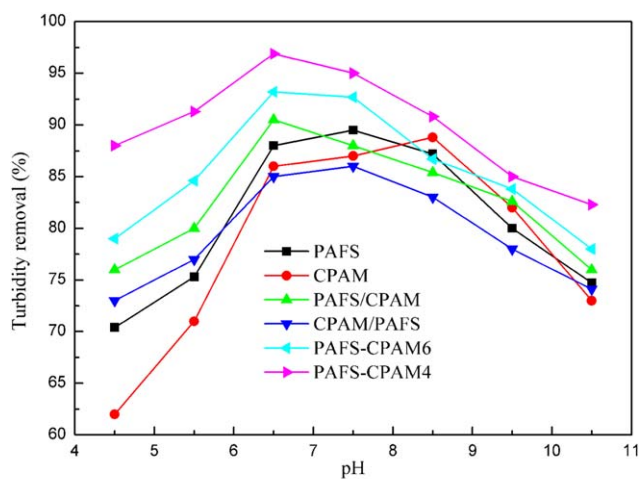
Nevertheless, the flocculation performance of PAFS–CPAM4 was better than the flocculation performance of PAFS–CPAM6. The best turbidity and COD removal rates of 95.6 and 86.3%, respectively, were obtained by PAFS–CPAM4 at 60 mg/L. Furthermore, PAFS–CPAM4 and PAFS–CPAM6 provided a turbidity removal rate of more than 80% and a COD removal rate of more than 75% within a broader dosage range compared with PAFS, CPAM, PAFS/CPAM, and CPAM/PAFS.

Removal efficiency decreased with increasing dosage. Gao et al.[21,22] obtained a similar result. The main reason for the decrease in flocculation efficiency was the overdosing effect of the flocculants. Two major mechanisms were involved in the flocculation of charged particles, namely, charge neutralization and adsorption bridging. When using CPAM or PAFS to flocculate negatively charged particles, charge neutralization was the dominant mechanism for PAFS, CPAM, and their dual flocculants. The surface charge of the particles reversed with increasing coagulant dosage, thus implying an electrostatic repulsion between the particles.

Effect of pH on Flocculation Efficiency

The effect of pH on the coagulation behavior of dual flocculants was examined in the range of pH 3.5 to pH 10.5 at a dosage of 60 mg/L. The turbidity and COD removal results are shown in Figures 5 and 6, respectively. Significant differences in turbidity and COD removal could be seen among PAFS, CPAM, and their dual flocculants. The removal ratios of the turbidity and COD by the investigated flocculants increased rapidly with the increasing initial pH of wastewater. When the pH was between 6.5 and 8.5, the turbidity and COD removal reached the maximum. However, the high pH was not favorable for the removal of turbidity and COD. Figure 6 shows that when the pH ranged from 3.5 to 7.5, the COD removal efficiency of PAFS/CPAM hardly changed. The flocculation efficiency of composite flocculants was better than that of the single flocculant.

Compared with CPAM, the COD removal efficiency of PAFS was much higher within the pH range of 6–9. The COD removal efficiency of dual flocculants, which was higher than
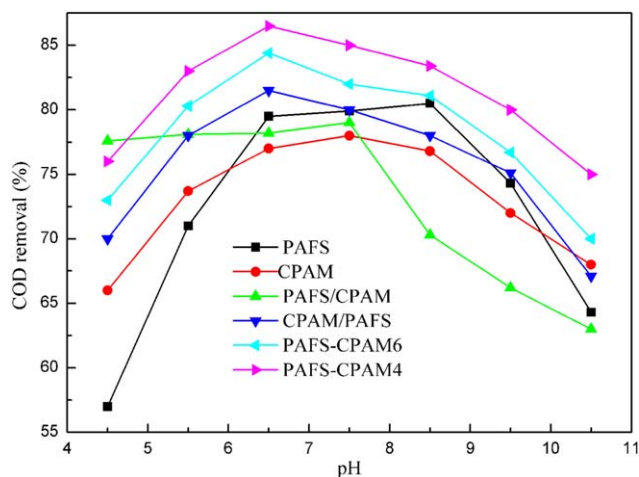
Figure 6. Effect of pH on COD removal. [Color figure can be viewed in the online issue, which is available at wileyonlinelibrary.com.]

Figure 7. Effect of settling time on turbidity removal. [Color figure can be viewed in the online issue, which is available at wileyonlinelibrary.com.]

80% in the pH range of 5–9, was slightly influenced by pH. All four dual flocculants performed better than PAFS and CPAM within most of the pH ranges investigated. The turbidity removal curves of the three dual flocculants showed similar trends. COD and turbidity removal rates of PAFS–CPAM6 and PAFS–CPAM4 increased and then slightly decreased with increasing pH. The optimal pH was 6.5. PAFS/CPAM, CPAM/PAFS, PAFS–CPAM6, and PAFS–CPAM4 achieved the optimal turbidity removal rate at pH of 6.5, 7.5, 6.5, and 6.5, respectively. At pH 7.5 and over pH 7.5, the COD removal rate of PAFS/CPAM was lower than the COD removal rates of CPAM/PAFS, PAFS–CPAM6, and PAFS–CPAM4. Figure 5 shows that the turbidity removal rates of two dual flocculants (i.e., PAFS–CPAM6 and PAFS–CPAM4) were higher than the turbidity removal rates of other flocculants in the acidic and neutral regions. However, the trends of their curves were similar. At pH 6.5, the order of turbidity removal was PAFS–CPAM4 > PAFS–CPAM6 > PAFS/CPAM > PAFS > CPAM > CPAM/PAFS, whereas the order of COD removal was AFS–CPAM4 > PAFS–CPAM6 > CPAM/PAFS > PAFS > PAFS/CPAM > CPAM.

The pH of wastewater directly affected not only the surface charge of colloidal particles but also the existing forms of the hydrolysis products of flocculants.[23] In the acidic condition, the stability and solubility of PAFS deteriorated, thus resulting in inefficient flocculation performance. Under an alkaline condition, PAFS was easily hydrolyzed and precipitated, thus leading to a low flocculation efficiency. CPAM was appropriate for a wide pH range and had a high adsorption-bridging ability, whereas PAFS had a high capacity for charge neutralization and netting sweeping. PAFS–CPAM was suitable for a wide pH range because of the advantages of PAFS and CPAM. The flocculation performance of polyferric (polyaluminum) flocculant strongly depended on Fe(III) and Al(III) hydrolysis species. $Fe_b(Al_b)$, which is the most active flocculating component in ferric (aluminum) salt coagulants, is responsible for flocculation performance.[24] In the current study, PAFS–CPAM provided the highest content of the active flocculating component $(Fe–Al)_b$ during coagulation. Furthermore, PAFS–CPAM provided higher
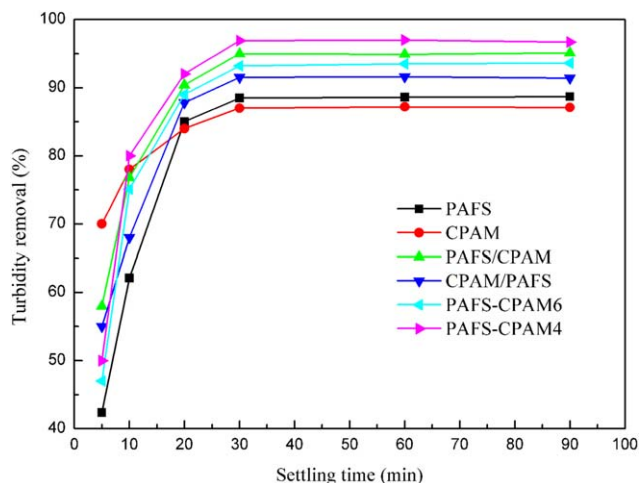
COD and turbidity removal rates than PAFS/CPAM and CPAM/PAFS (Figures 5 and 6). To obtain better flocculation efficiency, the optimum pH employed in this study was selected between 6.5 and 8.5.

Effect of Settling Time on Flocculation Efficiency
Settling time plays a significant role as an operating parameter in the practical applications related to the design size and investment cost of sedimentation tanks. Hence, the settling time was adopted as an index investigated in this study. Figures 7 and 8 show the effects of settling time on turbidity and COD removal. Both the turbidity and COD removal rates increased with increasing settling time. The removal rates stabilized when the settling time reached 20 min and remained the same after 30 min. The maximum COD removal rate had the following sequence: PAFS–CPAM4 > PAFS–CPAM6 > PAFS/CPAM > CPAM/PAFS > PAFS > CPAM. Therefore, the optimum settling time to employ in this research was fixed at 30 min.
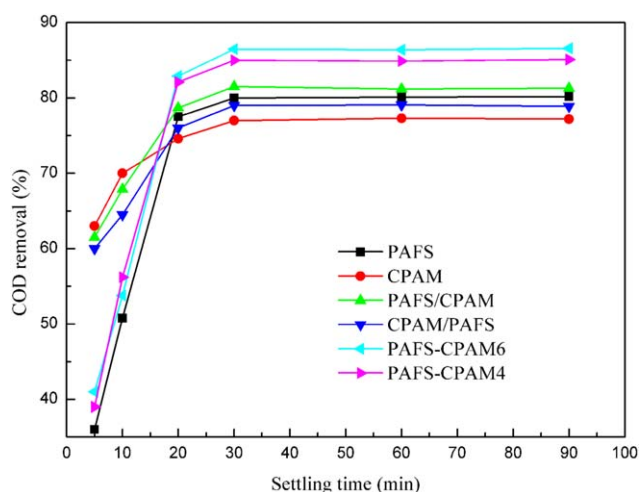

Figure 8. Effect of settling time on COD removal. [Color figure can be viewed in the online issue, which is available at wileyonlinelibrary.com.]
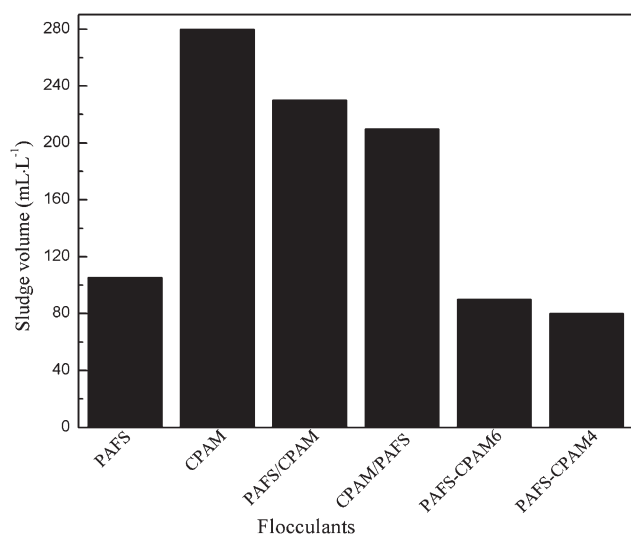
Figure 9. Sludge volume produced by different flocculants used for the optimal conditions.

Gao et al.[4] reported that the possible flocculation mechanisms of inorganic–organic composite flocculants in treating simulated dye water and actual textile wastewater were as follows. The average floc size flocculated by composite flocculants was larger than the average floc size of inorganic flocculants. The flocculation efficiency of PAFS–CPAM was higher than the flocculation efficiency of PAFS and CPAM in treating textile dye wastewater. PAFS–CPAM, PAFS, and CPAM removed turbidity and COD by adsorption/bridging, neutralization/bridging, and neutralization/bridging, respectively. In the current study, colloidal particles might be aggregated to micro-flocs by Fe(III) and Al(III) species in PAFS–CPAM. Thereafter, the micro-flocs might bridge together to form large flocs by the organic flocculants in PAFS–CPAM. The soluble dye was initially aggregated to an insoluble dye micro-compound by CPAM reaction, whereas the insoluble dye micro-compound was aggregated to large flocs by Fe(III) and Al(III) polymers. PAFS–CPAM produced the largest flocculant flocs with the fastest growth rate after rapid agitation at the beginning of flocculation. This result was in agreement with the conclusions of Wei et al.[25] and Gao et al.,[22] who found that the treatment of humic substances from water and actual textile wastewater by coagulation greatly depended on the neutralization of negative charges. In contrast, the bridging mechanism was unlikely to play a major part when cationic polymers were used as coagulants. Figure 7 shows that the turbidity removal rate flocculated by PAFS–CPAM4 and PAFS–CPAM6 were 93.6 and 96.7%, respectively, and Figure 8 shows that the COD removal rate flocculated by PAFS–CPAM4 and PAFS–CPAM6 were 85.1 and 86.6%, respectively. PAFS–CPAM formed a considerably larger and more compact floc structure and showed a faster settling rate than other flocculants.

Effect of Flocculants on Sludge Volume

The amount and characteristics of the sludge produced during the coagulation–flocculation process depend on the flocculants used and operating conditions.[26] In the current study, the sludge volume differed according to the flocculants used. The results obtained for the optimal conditions are shown in Figure 9.

The sludge volumes obtained by PAFS, CPAM, PAFS/CPAM, CPAM/PAFS, PAFS–CPAM6, and PAFS–CPAM4 were 105.6, 280.0, 230.0, 210.0, 90.0, and 80.0 mL/L, respectively. When PAFS–CPAM4 was used, the lowest sludge volume was obtained. This result supported the finding obtained in previous literature that the flocs produced by composite flocculants were compact and dense.[4,17] According to the discussion in "Effect of pH on Flocculation Efficiency" section, the main mechanisms for PAFS–CPAM, PAFS, and CPAM were charge neutralization/adsorption bridging, charge neutralization, and adsorption bridging, respectively. Previous studies[27,28] reported that the flocs produced by charge neutralization was always smaller than the floc produced by adsorption bridging. Thus, PAFS–CPAM not only improved treatment efficiency but also reduced sludge production compared with PAFS/CPAM, which used a different dosing method. In contrast, the use of a single flocculant (PAFS or CPAM) showed poor treatment efficiency.

CONCLUSIONS

The structure, species distribution, and flocculation behavior of composite flocculant PAFS–CPAM were investigated. The following conclusions were obtained:

1. FTIR analysis indicated that no new chemical bind was created when PAFS was combined with CPAM, thus implying that PAFS–CPAM was a physical mixture with a complex formation of PAFS and CPAM. SEM images showed that PAFS presented fluffy and wrinkled surface structures, which were favorable in coagulating colloidal particles and forming bridge aggregation among flocs compared with PAFS and CPAM. The synergy between PAFS and CPAM could also increase the $(Fe–Al)_b$ species of PAFS–CPAM. For the best flocculation behavior, the Fe–Al species distribution for PAFS–CPAM4 was improved by 42.85% with $(Fe–Al)_a$, 20.31% with $(Fe–Al)_b$, and 36.84% with $(Fe–Al)_c$.
2. Charge neutralization and adsorption are the main functions of turbidity and COD removal by PAFS–CPAM. PAFS–CPAM provided higher turbidity and COD removal performances depending on its sweep and bridging ability than PAFS/CPAM and CPAM/PAFS. The maximal flocculation efficiency (96.7% turbidity removal rate and 86.6% COD removal rate) was obtained by PAFS–CPAM at a dosage of 60 mg/L and pH 6.5 after 30 min settling time. PAFS–CPAM effectively reduced sludge volume after flocculation, thus reducing the sludge handling cost.

REFERENCES

1. Nguyen, T. A.; Juang, R. S. *Chem. Eng. J.* **2013**, *219*, 109.

2. Zheng, H. L.; Zhu, G. C.; He, Q.; Hu, P.; Jiao, S. J.; Tshukudu, T.; Zhang, P. *Water. Sci. Technol.* **2010**, *62*, 829.

3. Verma, A. K.; Dash, R. R.; Bhunia, P. *J. Environ. Manag.* **2012**, *93*, 154.

4. Gao, B. Y.; Wang, Y.; Yue, Q. Y.; Wei, J. C.; Li, Q. *Sep. Purif. Technol.* **2008**, *62*, 544.

5. Matilainen, A.; Vepsäläinen, M.; Sillanpää, M. *Adv. Colloid Interface* **2010**, *159*, 189.

6. Lee, K. E.; Morad, N.; Teng, T. T.; Poh, B. T. *Chem. Eng. J.* **2012**, *203*, 370.

7. Zhu, G. C.; Zheng, H. L.; Chen, W. Y.; Fan, W.; Zhang, P.; Tshukudu, T. *Desalination* **2012**, *285*, 315.

8. Zhu, G. C.; Zheng, H. L. Zhang, Z.; Tshukudu, T.; Zhang, P.; Xiang, X. Y. *Chem. Eng. J.* **2011**, *178*, 50.

9. Hu, Y. Y.; Tu, C. Q.; Wu, H. H. *J. Environ. Sci.* **2001**, *13*, 418.

10. Zhou, W. Z.; Gao, B. Y.; Yue, Q. Y.; Liu, L. L.; Wang, Y. 2006. *Colloids Surf. A* **2006**, 278, 235.

11. Zhu, J. R.; Zheng, H. L.; Jiang, Z. Z.; Zhang, Z.; Liu, L. W.; Sun, Y. J.; Tshukudu, T. *Desalin. Water Treat.* **2013**, *51*, 2791.

12. Zheng, H. L.; Jiao, S. J.; He Q.; Chen R.; Zhang P.; Fang H. L. *Spectrosc. Spectral Anal. (in Chinese)* **2011**, *31*, 551.

13. Noppakundilograt, S.; Nanakorn, P.; Sonjaipanich, K.; Seetapan, N.; Kiatkamjornwong, S. *J. Appl. Polym. Sci.* **2009**, *114*, 2564.

14. Noppakundilograt, S.; Nanakorn, P.; Jinsart, W.; Kiatkamjornwong, S. *Polym. Eng. Sci.* **2010**, *50*, 1535.

15. Zheng, H. L.; Zhu, G. C.; Jiang, S. J.; Tshukudu, T.; Xiang, X. Y.; Zhang, P.; He, Q. *Desalination* **2011**, *269*, 148.

16. Ma, J. Y.; Zheng, H. L.; Tan, M. Z. Liu, L. W.; Chen, W.; Guan, Q. Q.; Zheng, X. K. *J. Appl. Polym. Sci.* **2013**, *129*, 1984.

17. Gao, B. Y.; Wang, Y.; Yue, Q. Y. *Acta Hydrochim. Hydrobiol.* **2005**, *33*, 365.

18. Zhu J. R.; Zheng, H. L.; Zhang, Z.; Jiang, Z. Z.; Guan, Q. Q.; Tan, M. Z.; Dai, L.; Chen, W. *CIESC J.* **2012**, *63*, 4019.

19. Tzoupanos, N. D.; Zouboulis, A. I. *Water Res.* **2011**, *45*, 3614.

20. Cai, Z. S.; Yang, C. S.; Zhu, X. M. *J. Appl. Polym. Sci.* **2010**, *118*, 299.

21. Wei, J. C.; Gao, B. Y.; Yue, Q. Y.; Wang, Y.; Lu, L. *J. Hazard. Mater.* **2009**, *165*, 789.

22. Gao, B. Y.; Wang, Y.; Yue, Q. Y.; Wei, J. C.; Li, Q. *Sep. Purif. Technol.* **2007**, *54*, 157.

23. Shukla, N. B.; Madras, G. *J. Appl. Polym. Sci.* **2013**, *127*, 2251.

24. Kaemkit, C.; Monvisade, P.; Siriphannon, P.; Nukeaw, J. *J. Appl. Polym. Sci.* **2013**, *128*, 879.

25. Wei, J. C.; Gao, B. Y.; Yue, Q. Y.; Wang, Y.; Li, W. W.; Zhu, X. B. *Water Res.* **2009**, *43*, 724.

26. Aguilar, M. I.; Sáez, J.; Lloréns, M.; Soler, A.; Ortuño, J. F.; Meseguer, V.; Fuentes, A. *Chemosphere* **2005**, *58*, 47.

27. Yang, Z.; Yuan, B.; Huang, X.; Zhou, J. Y.; Cai, J.; Yang, H.; Li, A. M. Cheng, R. S. *Water Res.* **2012**, *46*, 107.

28. Liu, R.; Chiu, H. M.; Shiau, C. S.; Yeh, R. Y. L.; Hung, Y. T. *Dyes Pigments* **2007**, *73*, 1.